

# LINEAR FRICTION WELDING OF ALLVAC<sup>®</sup> 718 PLUS SUPERALLOY

K.R. Vishwakarma<sup>1</sup>, O.A. Ojo<sup>1</sup>, P. Wanjara<sup>2</sup>, M.C. Chaturvedi<sup>1</sup>

<sup>1</sup>Department of Mechanical and Manufacturing Engineering, University of Manitoba;  
75A Chancellors Circle, Winnipeg, Manitoba, R3T 5V6, Canada

<sup>2</sup>National Research Council Canada, IAR-AMTC, Montreal, PQ, H3T 2B2, Canada

Keywords: ALLVAC 718 Plus, Linear Friction Welding, Intergranular liquation

## Abstract

Linear Friction Welding (LFW) process was used to join Allvac<sup>®</sup>718 Plus (718 Plus) superalloy and produce a sound weld that was free of cracks both after welding and post weld heat treatment (PWHT). However, contrary to that reported in literature, it was found that the friction welding was not a completely solid state joining process as a significant grain boundary liquation was observed in the thermo-mechanically affected zone (TMAZ) of the welded material. The intergranular liquation was due to constitutional liquation of second phase particles like MC type carbides, Ti rich carbonitride particles and  $\delta$  phase precipitates. Liquation resulted in formation of Laves phase particles during welding and a non-uniform distribution of the main strengthening phase of the alloy,  $\gamma$  precipitates, during PWHT. Despite considerable liquation, there was no intergranular microfissuring which might be related to the nature of imposed stress during the LFW process.

## Introduction

Linear friction welding (LFW) offers an attractive alternative to the conventional welding processes used for manufacturing and repair of aerospace components. Like other frictional welding processes, it involves joining of components using frictional heat produced by their relative motion and forging pressure. It can be broadly classified into four distinctive steps as outlined by Vairis et al. [1] – (a) the initial stage where sufficient heat is generated due to solid friction; (b) the transition stage where the contact moves beyond the interface expelling the asperities; (c) the equilibrium stage which involves further generation of heat and joining at the interface and (d) the deceleration stage where the movement of the components is stopped with application of a forging pressure. The resulting microstructure consists of the weld center; the thermo-mechanically affected zone (TMAZ) and the unaffected base metal. Depending on the position in the weldment, different regions of the TMAZ and the base metal are subjected to different ranges of temperatures and plastic deformation that influence microstructural development.

LFW is generally considered a completely solid-state joining process, which like other friction welding processes could eliminate problems associated with melting and re-solidification of conventional fusion welding techniques. LFW has been successfully used to join steel, aluminum, titanium and intermetallic alloys [2, 3] in applications including manufacturing and repair of turbine components. It has also been used to weld dissimilar polycrystalline [4] and single crystal materials [5].

In the current investigation, Ni-based superalloy Allvac 718 Plus, principally strengthened by  $\gamma'$ , was used. 718 Plus is a comparatively new superalloy based on widely used Inconel 718, but can be used up to a working temperature of 700°C instead of 650°C, which is the highest temperature at which Inconel 718 can be used [6]. A previous study showed that the alloy cracked during conventional welding, as well as during the subsequent post weld heat treatment (PWHT) [7]. The present study was initiated to examine the viability of using LFW technique to weld 718 Plus alloy and to study the microstructure developed during welding and PWHT.

## Experimental

The as-received 718 Plus alloy was in the form of 15.9 mm×304.8 mm×127 mm hot rolled plates with a chemical composition of (wt.%) 17.92 Cr, 9.00 Co, 52.18 Ni, 9.33 Fe, 1.50 Al, 0.74 Ti, 5.51 Nb, 2.68 Mo, 1.04 W, 0.003 B (30 ppm), and 0.006 P (60 ppm). The as-received microstructure consisted of FCC  $\gamma$  matrix with randomly dispersed second phase particles including MC type carbides, Ti rich carbonitrides and  $\delta$  phase precipitates. 12.8 mm × 11.1mm × 17.7 mm test coupons were machined from the as-received plates and were solution treated at 950°C for 1 hour followed by water quenching. Prior to welding, the contact surfaces of the coupons were ground and cleaned with alcohol. LFW was performed at ambient temperature under prevailing atmospheric conditions using a MTS Linear Friction Welding Process Development System (PDS) located at the National Research Council of Canada's Institute for Aerospace Research. Details on the technical specification of the equipment are described elsewhere [8]. Previous work on LFW of Inconel 718 using processing conditions of 80 Hz for the frequency (f), 2 mm for the amplitude (a), 70 MPa for the forging pressure (P) and 2 mm for the axial shortening (s) indicated that only the center section of the welded coupons was bonded [9]. To extend bonding to the periphery regions, the frequency was increased to 100 Hz and the pressure to 90 MPa in the present work for LFW of the 718 Plus.

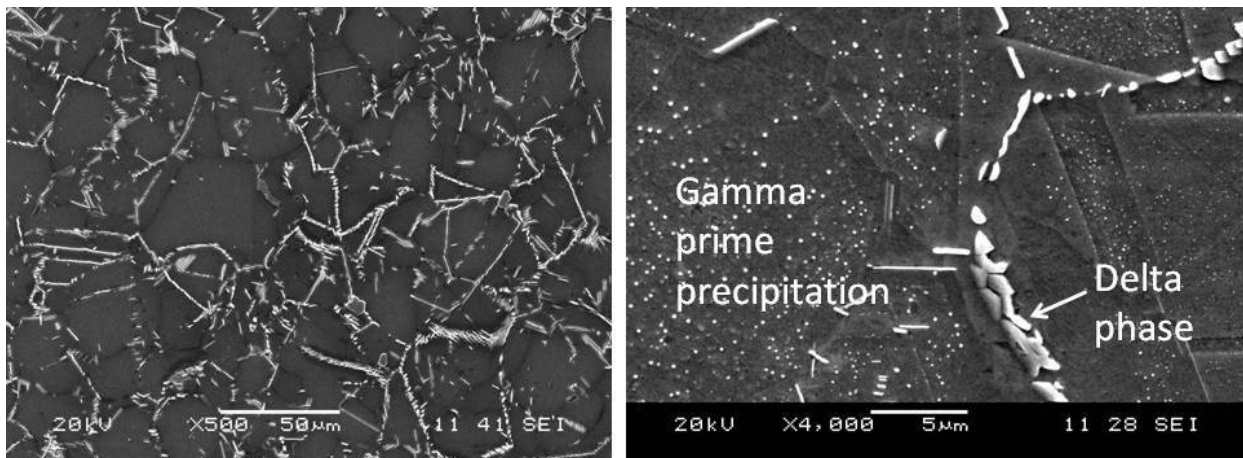


Figure 1: a) Low mag. and b) high mag. SEM image of as-welded base metal microstructure

The as-solutionized microstructure of the alloy consisted of an austenitic matrix and secondary precipitates as shown in Figures 1a and 1b. The precipitates were identified based on their morphology and SEM/EDS analysis [7]. The orthorhombic  $\delta$  phase was mostly present at the grain boundaries, with either small or large needle like morphology or in the platelet form. Round and blocky Nb rich MC type carbides and Ti rich carbonitride particles were randomly distributed throughout the microstructure. SEM analysis also revealed a uniform distribution of  $\gamma'$ , which is the principal strengthening phase in this alloy (Figure 1b). Welded specimens were

subjected to the standard PWHT, which consisted of treatment at 950°C for 1 hour followed by air cooling, aging at 718°C for 2 hours and then at 650°C for 8 hrs followed by air cooling. Cross-sections of the as-welded and post weld heat treated samples in the long transverse direction were used for microstructural analysis. Metallographic specimens were etched by modified Kalling's reagent and electrolytically in 10% oxalic acid. Samples were also electrolytically etched in a mixture of 12 mL H<sub>3</sub>PO<sub>4</sub> + 40 mL HNO<sub>3</sub> + 48 mL H<sub>2</sub>SO<sub>4</sub> at 6V for 5-6 seconds to reveal  $\gamma'$  phase in the microstructure. The fusion zone, base metal and TMAZ microstructures were examined and analyzed using an optical microscope and JEOL 5900 scanning electron microscope (SEM) equipped with an ultra thin window Oxford energy dispersive spectrometer (EDS).

## Results and Discussion

The LFW technique produced a sound and crack-free weld in the 718 Plus alloy. Figure 2 shows a low magnification optical micrograph of the microstructure of the as welded 718 Plus alloy. Three different zones can be observed in the micrograph – the base metal, thermo-mechanically affected zone (TMAZ) and the weld center.

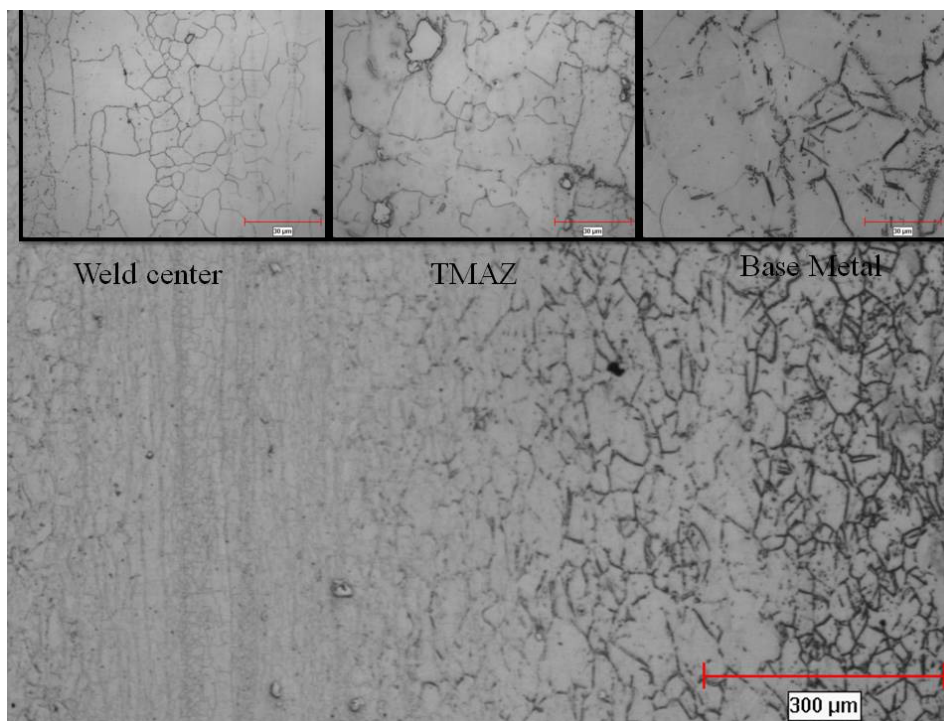


Figure 2: Microstructure of the LFWelded 718 Plus superalloy showing the weld center, TMAZ and the base metal

The weld center consisted of very fine grains and precipitate-free grain boundaries without any microfissuring in it. The most striking feature of the weld center was the change in grain size. A comparison of the grain sizes in the base metal and that in the weld center is shown in an optical micrograph in Figure 3. Particularly, over a region of about 30 μm from the weld line, the grain size was significantly smaller (less than 10μm) as compared to that in the base metal (average 50μm). The fine grain size is a characteristic feature of the linear friction welds, which has been also observed in Ti base alloys as well as Inconel 718 [8, 9], and has been suggested to be a result of dynamic recrystallization occurring during the joining process. The occurrence of

dynamic recrystallization has been attributed to the thermomechanical conditions imposed during LFW that involve a combination of high strains at elevated temperatures and high strain rates. Beyond 30  $\mu\text{m}$  from the weld line, the grain size increased progressively in size, inevitably due to the gradients in temperature and strain rate. At about 100  $\mu\text{m}$  from the weld line the average grain size in the TMAZ was similar to that of the base metal. It is noteworthy that in the weld center region no resolidified products were observed and, except for a few carbides, the other secondary phases like  $\delta$  phase and  $\gamma$  precipitates were not observed. Also, in comparison to previous work on Inconel 718 [9], the present processing conditions of higher frequency and pressure were capable of achieving an integral weld along the entire cross-section of the joint without the presence of residual oxide particles along the weld line.

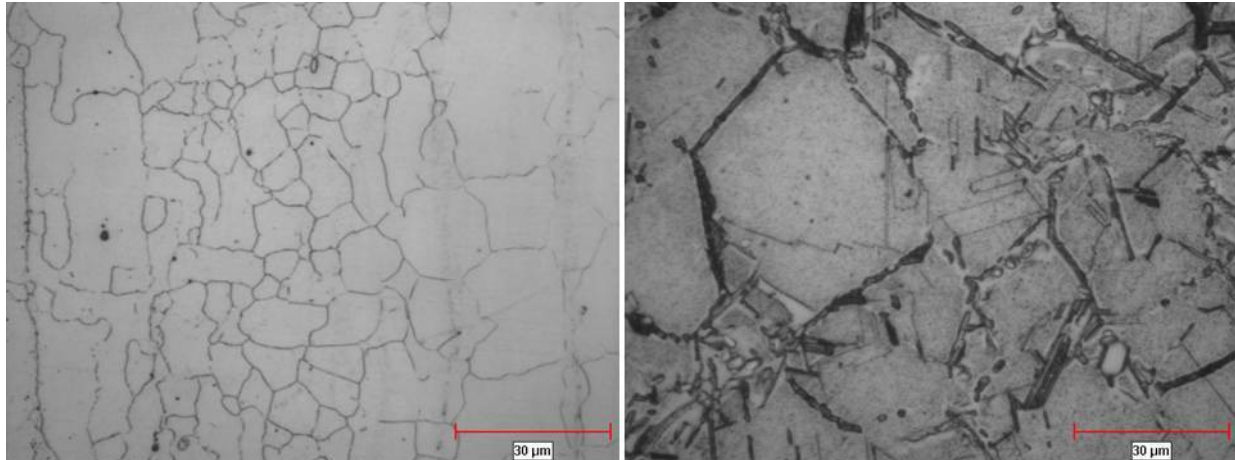


Figure 3: Recrystallized grains at the weld center and grains in the base metal – both figures have the same magnification

Liquation is generally not expected during solid state joining processes like LFW because the temperature reached during the process is believed to be below the solidus temperature of the alloy. However, sub solidus liquation can occur by non-equilibrium process. Possible causes of sub-solidus liquation are constitutional liquation of second phase particles and lowering of the melting point due to segregation of melting point depressants. Constitutional liquation was first proposed by Pepe and Savage in 1967 [10]. Consider the hypothetical eutectic diagram shown in Figure 4, where an alloy with a composition  $C_1$  is heated at a very slow rate to above the solvus temperature  $T_V$ , to a single phase,  $\alpha$  region. At  $T_V$ ,  $A_xB_y$  particles will be completely dissolved by solid-state diffusion to give a homogenous  $\alpha$  solid-solution. However, when alloy  $C_1$  is heated rapidly above  $T_V$ , as often is the case in welding,  $A_xB_y$  precipitates may not have enough time to dissolve completely in the  $\alpha$  matrix because of the slow solid-state diffusion process. Upon heating to the eutectic temperature  $T_E$ , the residual  $A_xB_y$  particles would react with the surrounding  $\alpha$  matrix to form a liquid phase with composition  $C_E$  at the particle/matrix interface. Hence, localized melting is possible below the equilibrium solidus temperature  $T_S$ , when rapid heating rate is involved.

Constitutional liquation of second phase particles during conventional welding processes has been observed in several nickel base alloys including 718 Plus alloy, however occurrence of the same in LFW has not been reported. The heating rate involved during LFW has been suggested to be as high as 280°C/s [9] which can induce non-equilibrium liquation of second phase particles. In the present work, intergranular and intragranular liquation was observed in the TMAZ of LFWed 718 Plus as shown in Figure 5. Whereas all the grain boundaries in the TMAZ

appeared liquated, a few of these grain boundaries, as marked “A” in Figure 6, are conspicuously different with a wavy pattern of solidification. The zigzag nature of these grain boundaries is typical of “liquid film migration (LFM)”. It was also observed that these grain boundaries with LFM feature were devoid of any resolidified products, unlike other grain boundaries in the TMAZ (marked “B”). LFM has been observed in the HAZ of several Ni-base superalloys welded by conventional fusion welding techniques [11-13]. Under certain conditions, liquated regions of the HAZ in these alloys can solidify via LFM. It has been observed that, depending on the thickness of the liquated grain boundary and the concentration of the liquid, the normal solidification mode resulting in formation of resolidified products can be replaced by liquid film migration, which is a faster solidification process [12].

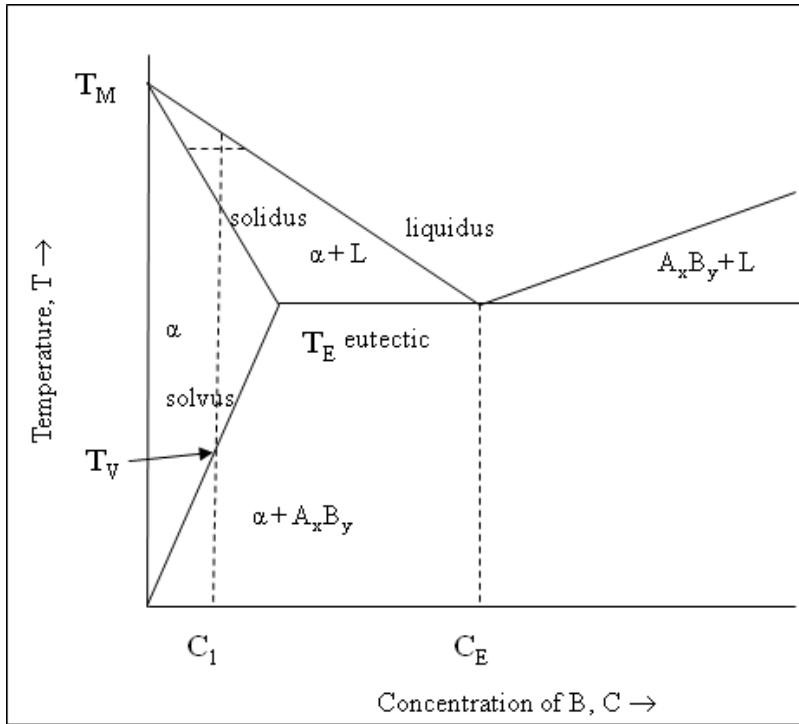


Figure 4: Hypothetical binary phase eutectic diagram

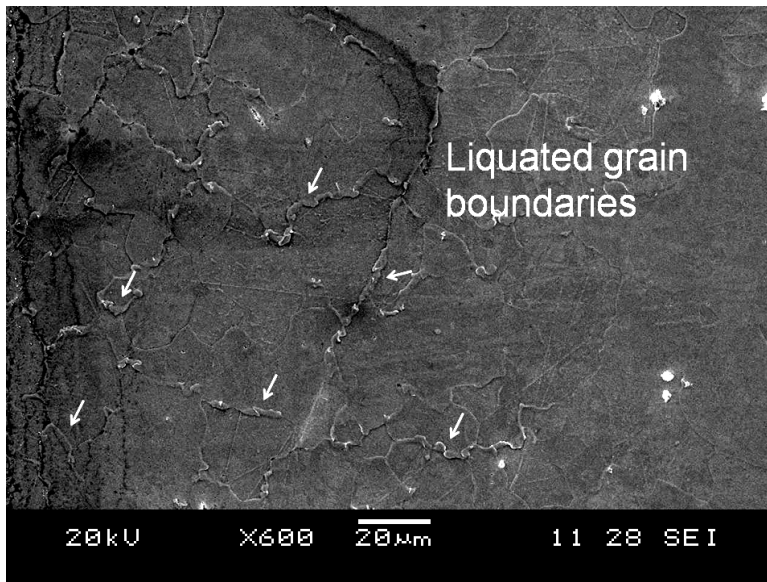


Figure 5: Grain boundary liquation in TMAZ of as welded 718 Plus linear friction weld

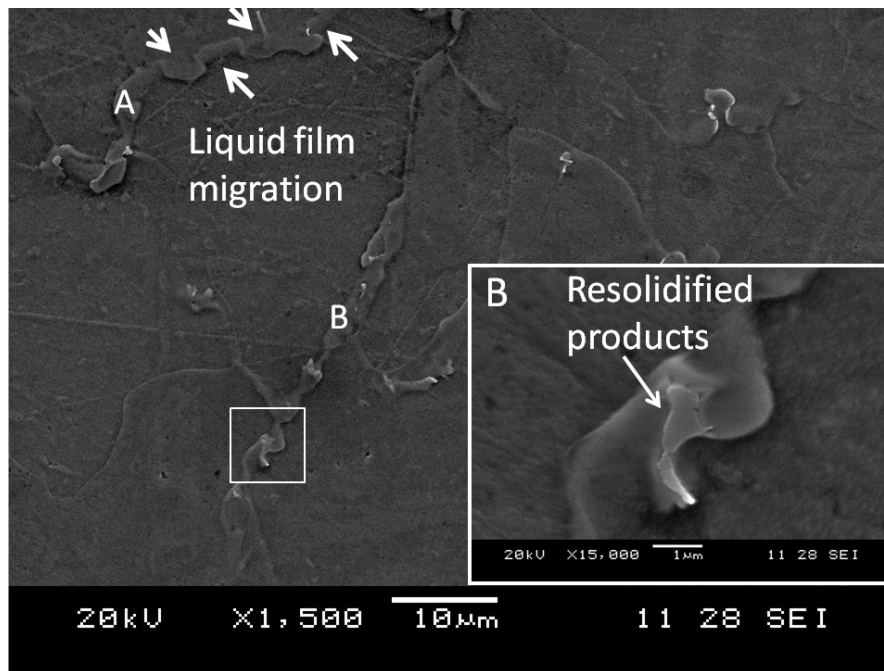


Figure 6: Evidence of liquid film migration and resolidified products on the liquated grain boundaries in the as-welded microstructure

Grain boundaries such as those marked “B” in Figure 6 were carefully analyzed using SEM EDS analysis in order to identify the resolidified products. Table 1 shows the chemical composition of resolidified product as determined by SEM EDS analysis. As can be seen from the data presented, these products have distinctively different chemical composition from that of carbides and carbonitride particles. The chemistry of resolidified product is similar to that of  $\delta$  phase and Laves phase, both of which have a similar chemical composition, however, the morphology of the resolidified product is different from that of  $\delta$  phase but is consistent with that of the Laves phase [7]. Therefore, based on the chemical analysis and morphology, the resolidified products are suggested to be Laves phases. Figure 7 shows one such Laves phase and the corresponding EDS analysis spectrum. Laves phase has a hexagonal closed packed structure, and it usually forms in Inconel 718 type of alloys during solidification. In an earlier physical metallurgical analysis of 718 Plus alloys, Laves phases were not observed in wrought alloys [7], however, Laves phase can form by solidification reaction during conventional arc welding. Hence based on the above discussion Laves phase in the LFW of 718 Plus could have been produced by liquation and solidification in the form of Laves +  $\gamma$  eutectic. Solidification in Inconel 718 and 718 Plus alloys is generally believed to terminate by  $\gamma$  + Laves eutectic reaction [14, 15]. The  $\gamma$  phase from the Laves +  $\gamma$  eutectic, blends with the primary matrix, although a halo indicative of the resolidified  $\gamma$ , can be observed around the Laves phase separating it from prior  $\gamma$  matrix as seen in the Figure 7. Formation of Laves phase has been found to be detrimental to the mechanical properties of the alloy due to their brittle nature [16]. However, it is to be noted that Laves phase forms in the weld zone in conventionally welded wrought Inconel 718 whereas, no Laves phase was observed in the weld center in LFW 718 Plus alloy.

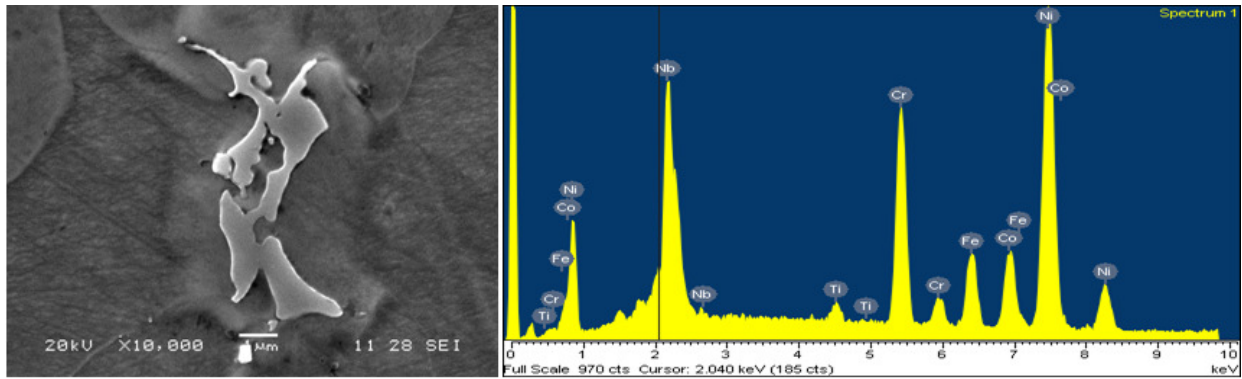


Figure 7: Resolidified constituent identified as Laves +  $\gamma$  eutectic at the grain boundary

Table 1: Average chemical composition of the second phase particles and matrix as determined by SEM EDS analysis in 718 Plus alloy

wt%	NbC	Ti(C,N)	Laves phase	Delta phase	Matrix	Particles at the weld center after PWHT
Al			1	2	1	1
Ti	8	63	5	1	1	3
Cr	1	5	16	17	18	10
Fe		2	8	9	9	5
Co			9	10	10	8
Ni	2	10	50	55	53	57
Nb	89	20	11	6	4	16
Mo				3	3	
W			2	1	1	2

Liquation in the TMAZ also occurred by constitutional liquation of Nb rich MC type carbides and Ti rich carbonitride particles. Figures 8 and 9 show the backscattered images of Nb rich MC type carbides and Ti rich carbonitride particles, with their EDS spectra, respectively. The constitutionally liquated carbides and carbonitride particles were different in appearance from those present in the base metal. The particles in the base metal exhibited a well defined solid edge whereas those in the TMAZ had serrated interface which is typical of liquated particles. Constitutional liquation of carbides and carbonitrides is a well established phenomenon in conventional fusion welding of 718 type of superalloys. Similar features associated with grain boundary liquation cracking in 718 Plus were observed in an earlier investigation by the present authors on electron beam welding of 718 Plus alloy [7, 17]. The characteristics of liquation and the resolidified products in LFWed 718 Plus are observed to be comparable to those observed in the EB welds [17], although the liquation did not result in microfissuring in the LFWed material. Occurrence of grain boundary liquation is not a sufficient condition to determine susceptibility for weld intergranular cracking. Generation of sufficient tensile stresses at a time when the grain boundary regions are weakened by the presence of liquid phase is necessary to cause cracking by decohesion along one of the solid-liquid interfaces. Preclusion of intergranular cracking in the present work could be related to the imposition of compressive stress during the forging stage of the LFW, which essentially counters the driving force for cracking, that is, the tensile stress.

It is likely that a significant portion of the intergranular liquation occurred due to reaction involving  $\delta$  phase, which was present at the base metal grain boundaries prior to welding. The contribution of  $\delta$  phase to liquation has been reported in earlier studies in conventional Inconel 718 and 718 Plus alloy [18, 19]. It was proposed that  $\delta$  phase disassociated above its solvus (about 1010°C in Inconel 718) [20] and enriched the grain boundary with Nb, a melting point depressant, which lowered the melting point of the grain boundary material and caused liquation. This is called “ $\delta$  phase assisted liquation” [19]. However, recently, Zhang et al. [21] observed that  $\delta$  phase can actually constitutionally liquate in the HAZ of conventional Inconel 718 superalloy.

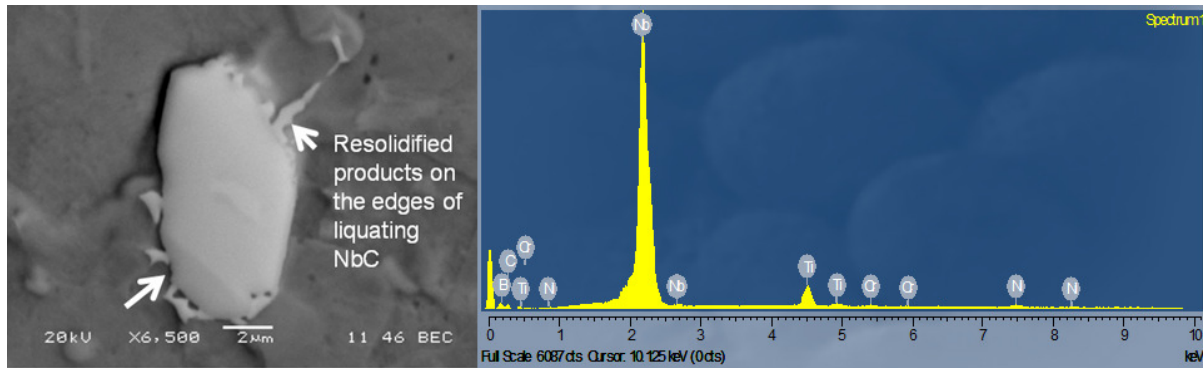


Figure 8: Constitutional liquation of MC type carbide and the associated EDS spectrum

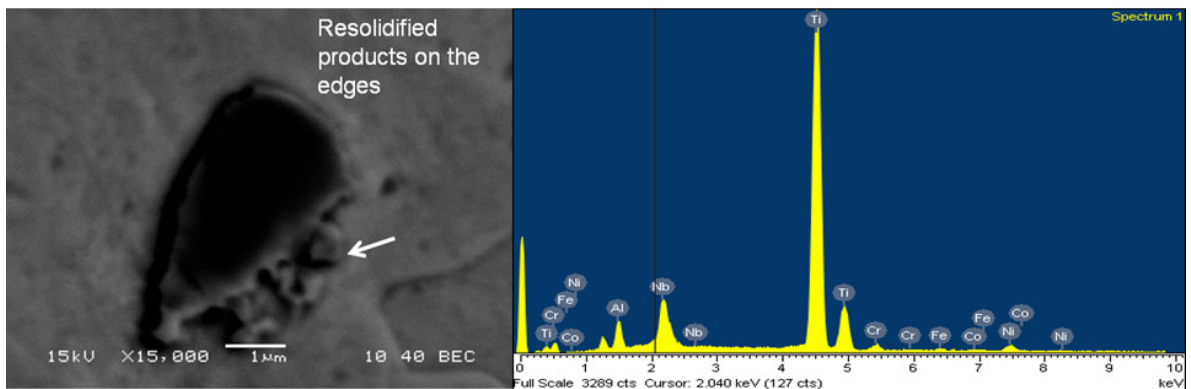


Figure 9: Inter granular liquation of Ti(C,N) particle in the TMAZ and its EDS spectrum

PWHT is generally aimed to homogenize the weld microstructure and the standard PWHT for 718 Plus alloy was used in the present work. Fine precipitates were observed at the grain boundaries of the material in the weld center after PWHT, as shown in Figure 10. These particles were found to be rich in Nb, however EDS analysis could not reveal the composition precisely due their fine size (Table 1). Further analysis is planned to determine the exact nature of these particles by HRTEM. As was the case in the as-welded condition, no microfissuring was observed in the post weld heat treated (PWHTed) LFWed 718 Plus alloy.

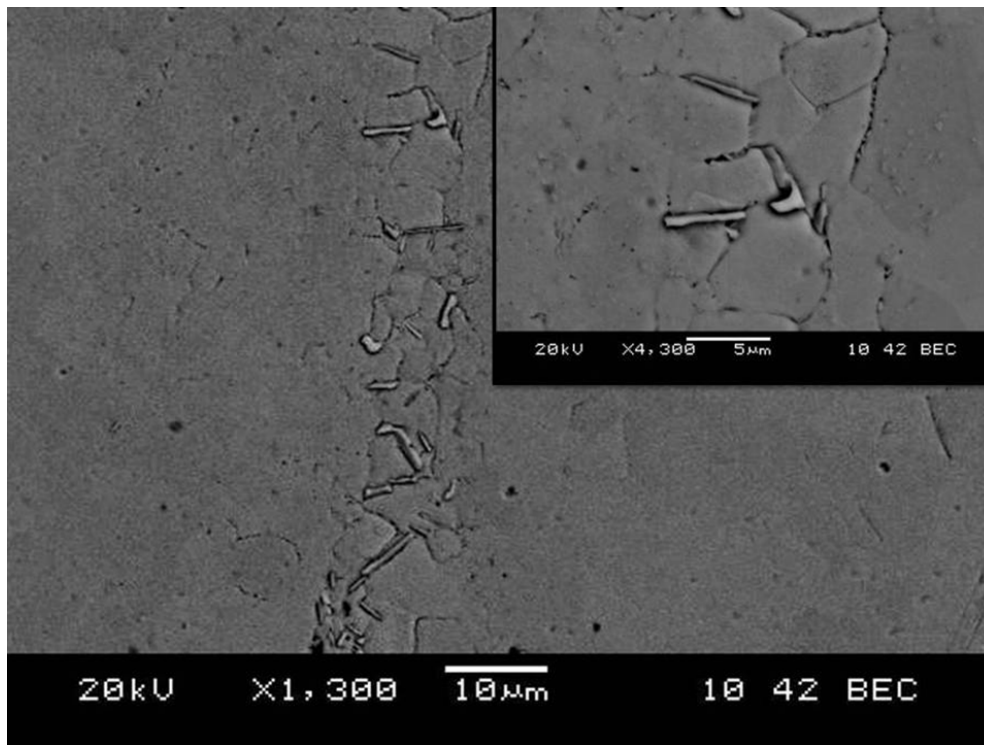


Figure 10: Fine intergranular precipitates at the weld center after PWHT

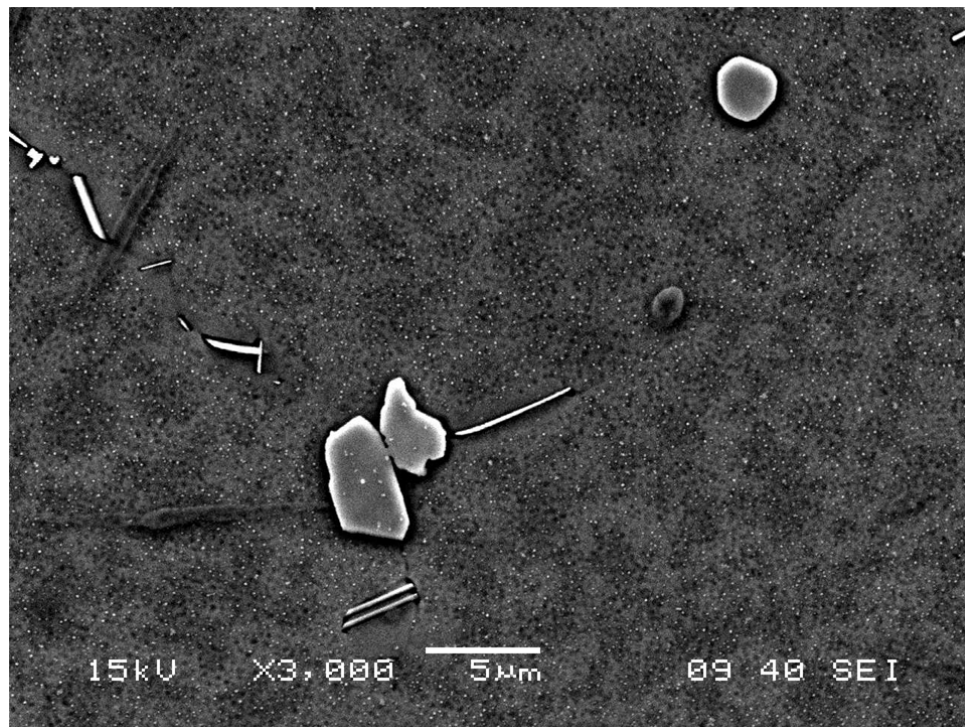


Figure 11: Base metal microstructure after PWHT

Figure 11 shows the base metal microstructure of PWHTed alloy 718 Plus consisting of coarse NbC particles and  $\delta$  phase at the grain boundaries with uniform distribution of  $\gamma$  precipitates. The transition from base metal to the TMAZ is apparent in the PWHTed samples by a change in the amount and distribution of second phase particles. Figure 12 shows a marked difference in the amount of  $\gamma$  particles between the TMAZ and base metal. It was observed that the

precipitation of  $\gamma$  in TMAZ was considerably less as compared to that in the base metal, and the distribution seemed to be non-uniform in nature. Similarly,  $\delta$  phase was also observed in smaller amounts as compared to that in the base metal and  $\delta$  phase particles were found to be more pronounced in the previously liquated and resolidified regions during welding. Figure 13 shows a grain boundary in the TMAZ region of the PWHTed sample showing clusters of precipitates on it. More precipitation was observed at prior liquated regions, i.e.; at the liquated grain boundaries and at constitutionally liquated carbides or nitrides.

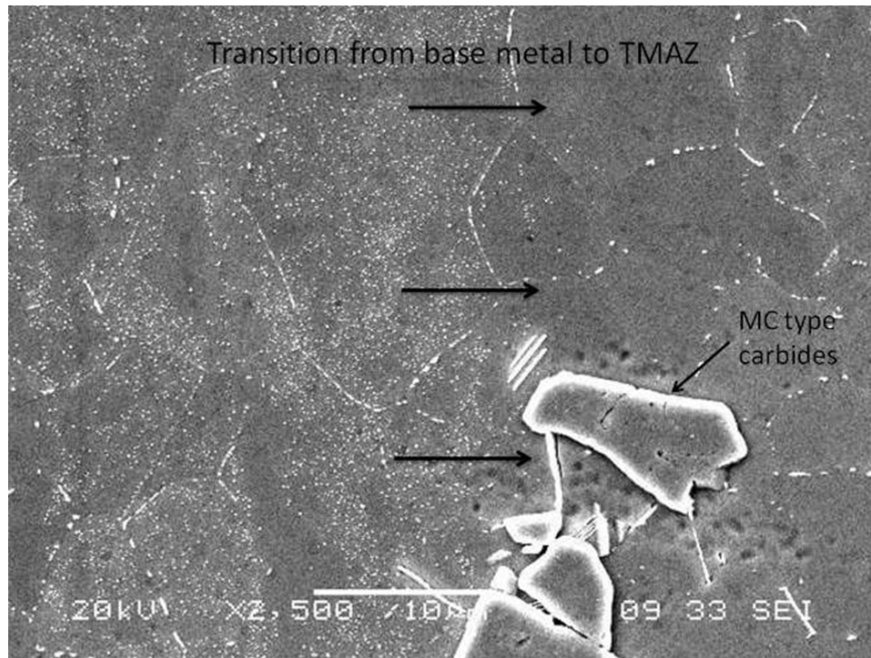


Figure 12: Transition from base metal to TMAZ microstructure in PWHTed alloy

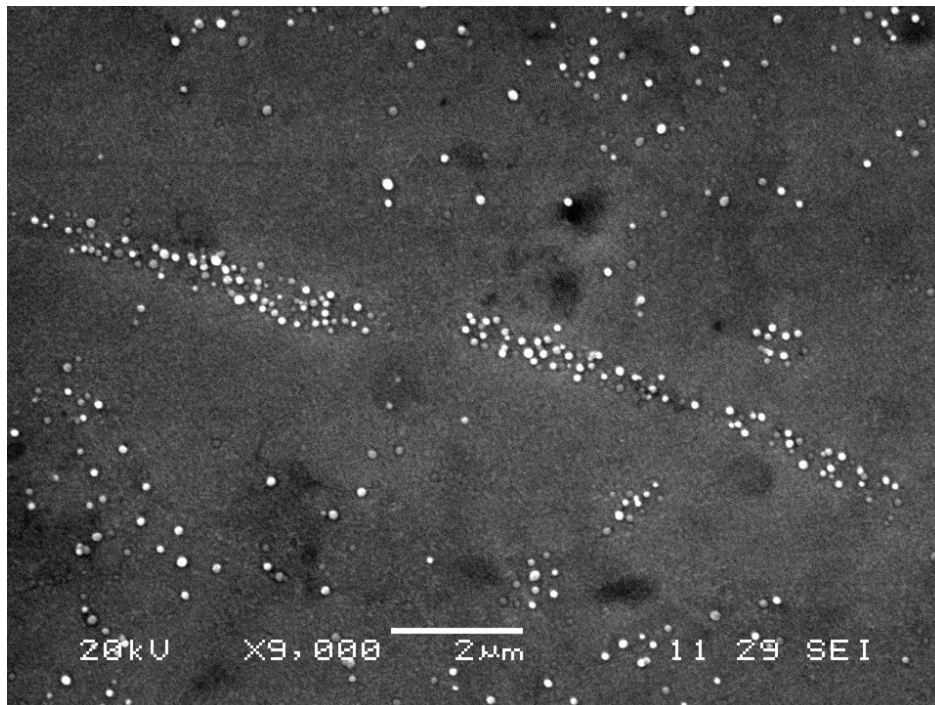


Figure 13: Non-uniform distribution of  $\gamma$  phase in the TMAZ of PWHTed 718 Plus weld

Laves phase particles that formed during the welding process were not eliminated by PWHT, rather they were surrounded by  $\delta$  phase precipitates, as observed in Figure 14. Similarly, such precipitation of  $\delta$  phase was observed around previously liquated carbides and carbonitride particles (Figure 15). Figure 15 also shows Laves phase on the edges of a liquated carbonitride particle. By comparing Figures 15 and 11 it is seen that, unlike in the TMAZ region, carbide and carbonitrides particles in the base metal did not have any Laves phase associated with them. This further indicates that liquation did occur during LFW in the TMAZ, because Laves phase in the 718 Plus alloy can only form by solidification of liquid phase in the microstructure.

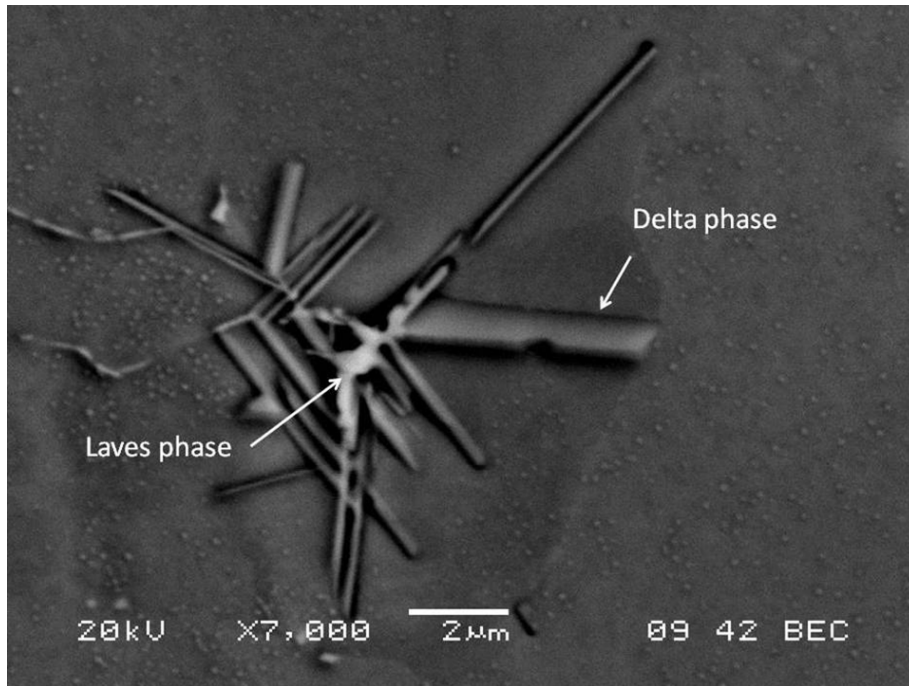


Figure 14: Laves phase and delta phase in the TMAZ after PWHT

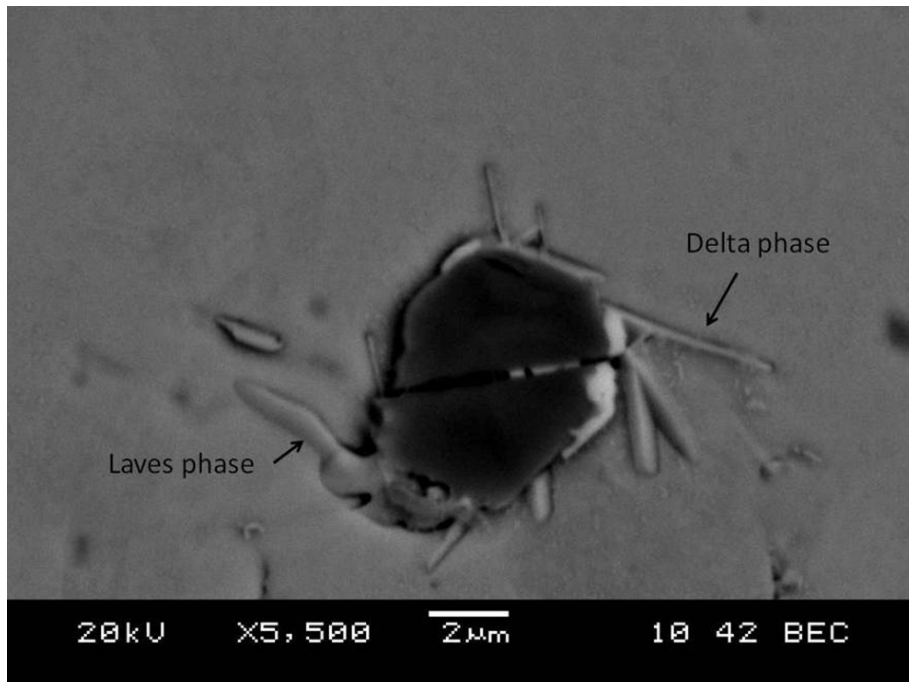


Figure 15: Ti carbonitride particles with  $\delta$  phase and Laves phase in the PWHTed condition

With the process parameters applied in the present work, it was shown that 718 Plus can be LFWed without cracking, even though liquation during welding resulted in formation of Laves phase during PWHT. Since the occurrence of liquation causes non-uniform precipitation of the main strengthening phase of the alloy,  $\gamma$  precipitate, further optimization of the critical processing parameters is indeed necessary. In addition, characterization of the mechanical performance in relation to the microstructural features of the as welded and PWHTed conditions will be essential for determining the impact of the liquation phenomenon and the ensuing Laves phase in causing micro-fissuring under the unique residual stress distribution of LFWed joints.

### Summary and Conclusions

1. Linear friction welding of Inconel 718 Plus at a frequency of 100 Hz, pressure of 90 MPa, amplitude of 2 mm and axial shortening of 2 mm was capable of generating an integral weld without oxide residue or particles at the weld line.
2. The weld region consisted of fine recrystallized grains and, though grain boundary liquation and constitutional liquation of second phase particles occurred in the thermomechanically affected zone, fissuring in the weldment was not observed.
3. Grain boundary liquation resulted in formation of Laves phase and inhomogeneous precipitation of the principle strengthening phase,  $\gamma$  during PWHT.
4. Laves phase, which are brittle in nature, could not be eliminated during PWHT. Also the standard PWHT could not homogenize the welded microstructure.
5. Notwithstanding the occurrence of liquation during welding and the formation of Laves phase during PWHT, microfissuring was not observed in the as welded and PWHT conditions, which may be attributed to the compressive stress state of the joint region during the forging phase of linear friction welding combined with the absence of resolidified products in the weld center.

### Acknowledgements

The authors would like to thank NSERC for all the financial support. The technical assistance of M. Guérin and E. Dalgaard for LFW of IN 718 Plus is also greatly appreciated.

### References

1. A.Varis and M.Frost, "Modelling the linear friction welding of titanium blocks", *Materials Science and Engineering A*, 292(2000), pp. 8-17.
2. M.Karadge, M.Preuss, C.Lovell and P.J.Withers, "Texture development in Ti-6Al-4V linear friction welds", *Materials Science and Engineering A*, 459 (2007), pp. 182-191.
3. A.Vairis and M.Frost, "High Frequency Linear Friction Welding of Titanium Alloy", *Wear*, 217 (1998), pp. 117-131.

4. S.V.Lalam, G.M. Reddy, T. Mohandas, M. Kamaraj and B.S.Murty, "Continuous drive friction welding of Inconel 718 and EN 24 dissimilar metal combination", *Materials Science and Technology*, 25 (2009), pp. 851-861.
5. M. Karadge, M. Preuss, P.J.Withers and S.Bray, "Importance of crystal orientation in linear friction joining of single crystal to polycrystalline nickel-base superalloys", *Materials Science and Engineering A*, 491 (2008), pp. 446-453.
6. W.D.Cao and R.Kennedy, "Role of chemistry in 718-type alloys - ALLVAC 718 PLUS TM alloy development", *Superalloys 2004*, (2004), pp. 91-99.
7. K.R.Vishwakarma, N.L. Richards and M.C. Chaturvedi, "Microstructural analysis of weld and heat affected zone of electron beam welded ALLVAC 718 PLUS TM Superalloy", *Materials Science and Engineering A*, 480 (2008), pp. 517-528.
8. P. Wanjara and M. Jahazi, "Linear friction welding of Ti-6Al-4V: Processing, Microstructure, and Mechanical-Property Inter-Relationships", *Metallurgical and Materials Transactions A*, 36A (2005), pp. 2149- 2164.
9. C. Mary and M.Jahazi, "Linear Friction Welding of IN-718 Process Optimization and Microstructure Evolution", *Advanced Materials Research*, 15-17 (2007), pp. 357-362.
10. J.J. Pepe and W.F.Savage, "Effects of constitutional liquation in 18-Ni Maraging Steel Weldments", *Welding Journal*, 9 (1967), pp. 411-s – 422-s.
11. O. Idowu, O.A. Ojo, and M.C. Chaturvedi, "Effect of heat input on heat affected zone cracking in laser welded ATI Allvac 718Plus superalloy", *Materials Science and Engineering A*, 454-455 (2006), pp. 389-397.
12. R. Nakkalil, N.L.Richards and M.C.Chaturvedi, "The influence of solidification mode on heat affected zone microfissuring in a nickel-iron base superalloy", *Acta Metallurgica et Materialia*, 41(1993), pp. 3381-3392.
13. O.A. Ojo, N.L.Richards and M.C.Chaturvedi, "Liquid film migration of constitutionally liquated gamma prime in weld heat affected zone (HAZ) of Inconel 738LC superalloy", *Scripta Materialia*, 51 (2004), pp. 141-146.
14. B. Radhakrishnan, and R.G.Thompson, "Solidification of the nickel-base superalloy 718 : A phase diagram approach", *Metallurgical Transactions A*, 20A (1989), pp. 2866-2868
15. B. Radhakrishnan and R.G.Thompson, "A model for the formation and solidification of grain boundary liquid in the heat affected zone (HAZ) of welds", *Metallurgical Transactions A*, 23A (1992), pp. 1783 – 1799.
16. J.J. Schirra, R.H. Caless, and R.W.Hatala, " The effect of Laves phase on mechanical properties of wrought and cast + HIP Inconel 718", *Superalloys 718, 625, 706 and various derivatives*, (1991), pp. 375 – 388.

17. K.R. Vishwakarma, N.L.Richards and M.C. Chaturvedi, "HAZ microfissuring in EB welded Allvac 718 Plus alloy" , *Superalloys 718, 625, 706 and various derivatives*,(2006), pp. 637-647.
18. Q. Li, "The influence of electron beam welding parameters on heat affected zone cracking in Allvac 718 Plus alloy", *Ph.D. Thesis, University of Manitoba*, (2006).
19. M. Qian and J.C. Lippold, "The effect of annealing twin-generated special grain boundaries on HAZ liquation cracking of nickel-base superalloys", *Acta Materialia*, 51 (2003), pp. 3351-3361.
20. S. Azadian, L.Wei and R.Warren, "Delta phase precipitation in Inconel 718", *Materials Characterization*, 57(2004), pp. 7-16.
21. H.R. Zhang and O.A.Ojo, "Non-equilibrium liquid phase dissolution of delta phase precipitates in a nickel based superalloy", *Philosophical Magazine Letters*, 89 (2009), pp. 787-794.